metals

Article

Mechanical Characterization of AA8006 Aluminum Alloy through Cold Free Forming Test

Gianluca Parodo *, Gillo Giuliano , Luca Sorrentino and Wilma Polini

Department of Civil and Mechanical Engineering, University of Cassino and Southern Lazio, 03043 Cassino, Italy; gillo.giuliano@unicas.it (G.G.); luca.sorrentino@unicas.it (L.S.); wilma.polini@unicas.it (W.P.)
* Correspondence: g.parodo@unicas.it

Abstract: In this work, for the first time thin, sheets of AA8006 aluminum alloy, that are commonly used for food packaging, were mechanically characterized through an unconventional free-forming technique that was performed at room temperature. This technique constitutes an economically effective solution to determine the constitutive equation of a metal sheet subjected to two-axes stresses. This state of stress reproduces the behavior of the material during the forming process better than the more traditional tensile test, which involves uniaxial stress. Specifically, the material constants were determined by using a simplified analytical model applied to the results of the experimental tests of the free forming process carried out at room temperature and constant pressure. Therefore, the obtained material constant values were used to simulate the same free-forming tests using FEM. In conclusion, the numerical results were in agreement with the experimental ones, thus confirming the goodness of the developed numerical model.

Keywords: free forming test; cold forming; ultra thin sheets; AA8006 aluminum alloy; finite element method

check for updates

Citation: Parodo, G.; Giuliano, G.; Sorrentino, L.; Polini, W. Mechanical Characterization of AA8006 Aluminum Alloy through Cold Free Forming Test. *Metals* **2023**, *13*, 1081. https://doi.org/10.3390/met13061081

Academic Editor: Hailin Yang

Received: 1 May 2023
Revised: 28 May 2023
Accepted: 6 June 2023
Published: 7 June 2023

1. Introduction

Metal sheets are traditionally formed by cold forming processes which involve a punch, a die, and a blank holder [1–4]. Cold forming manufactures different industrial products for the automotive industry (for example body parts), the household appliance industry (such as sinks, hoods, and freezers), or the food industry (for example cans, pots, and containers) [5–8]. Sheet metal forming allows obtaining by a metal sheet the final shape of the product by plastic deformation without involving machining processes. The sheet material can be steel, bronze, copper, brass, or aluminum alloys. Aluminum alloys are widely manufactured through cold forming because of their high deformability, good specific resistance, corrosion resistance, and weldability [9–12].

The use of aluminum alloys has shifted the interest of the industry towards hot metal sheet forming processes. This is because metal heating allows increasing their ductility to manufacture more complex shapes through a single forming step. This result was also achieved by using pressurized gas to replace the punch during the hot forming process. This approach is used in superplastic forming (SPF) that is carried out through blow forming or stretching processes that require the use of pressurized gas to replace the traditional punch [13–15]. The forming times are very long (tens of minutes) compared with those involved in the forming processes with a punch; thus the SPF processes used in industrial fields have a low production rate. However, faster blow forming processes have been investigated; they involve a lower process temperature and a higher value of the forming pressure [13–15].

In the aerospace, electronics, medical, and food packaging fields, the growing request for very thin parts has led to the development of reliable predictive numerical models to study manufacturing processes [3,16]. These models require knowing the mechanical behavior of the material under the load due to the manufacturing process. In fact, during forming, the deformation mechanisms of thin sheets are different from those with which the bulk properties of the material are obtained. Often, as the thickness of the sheet decreases, the formability of the material decreases. Chang et al. [17] described the effect of small thicknesses on the formability of carbon steel sheets. At the same size of the crystalline grain, thin sheets have a smaller number of grains along the thickness direction. This aspect leads to a lower ability to harden the material as the considered thickness decreases.

The mechanical behavior of the sheets is generally investigated by carrying out tensile tests. To characterize thin sheets, the results of the tensile tests depend on the cutting process adopted for manufacturing the specimens, because even small defects can generate non-negligible intensification of stress. For this reason, tensile tests on thin sheets require specific equipment to produce the specimens, such as ultraviolet laser cutting or double blade shears [18,19]. Trost et al. [18] used an industrial UV/CO_2 laser drilling machine for cutting very thin metallic foils to obtain dog bone specimens for tensile testing. The laser system allowed realizing a fine and repetitive pattern on the cutting edges, however, a localized heat affected zone (therefore a change in the structure of the material) was always present. Moreover, the tensile test submits the material to a uniaxial tension which differs from the tensions induced in the material during forming that are along multiple axes. An interesting alternative is a free-forming test that submits the material to biaxial tensions; therefore, the mechanical behavior of the material connected with the two tests is different. Therefore, the tension distribution obtained by the free forming test being nearer to those involved in the typical sheet forming processes of industrial interest, it is possible to state that mechanical parameters due to a free forming process are more representative of the material mechanical behavior [20]. Currently, there are no works of the literature that investigate the cold-free forming of thin metal sheets that are carried out with the blow forming technique. This technique to form very ductile and thin sheets allows them to be formed avoiding friction between sheet and punch [21,22]. This work presents the blow forming process applied for the first time to thin sheets of AA8006 aluminum alloy to mechanically characterize them. It represents a simple and economical solution to mechanically characterize thin sheets; thus, overcoming the problems connected with tensile tests.

2. Materials

This work uses thin sheets of 105 µm thickness in EN AW 8006 aluminum alloy. Table 1 shows the chemical composition of this alloy in wt%. Following the UNI EN 546-2 standard, the material has a tensile strength between 90 MPa and 150 MPa with a minimum elongation at a break of 15%.

Table 1. Chemical composition in wt% of EN AW 8006 aluminum alloy.

Elements	Percentage
Si	0.4
Fe	1.2–2.0
Cu	0.3
Mn	0.3–1.0
Mg	0.1
Zn	0.1
Al	Rest

3. Theory: Analytical Modelling of the Free Forming Process

The analytical modelling of the free forming process was first described in [23], where it was applied to the hot forming of superplastic sheets. The first experimental validations of hot forming for high-temperature superplastic materials were presented in [24]. Some authors have subsequently taken up the model by modifying some basic hypotheses (i.e., the non-constant thickness) [25,26]. A mathematical model was proposed in [27];

it uses the finite difference method and considers a non-uniform thinning of the sheet during the free-forming process of superplastic materials. In [13], there is a review of the mathematical modelling of the free-forming process for superplastic materials. The finite element model was used to determine the constants of different superplastic materials [28], such as the Ti6Al4V alloy [29], the AZ31 magnesium-based alloy [30], and the AA5083 [31] and AA2017 [15] aluminum alloys.

Figure 1 shows the scheme of the process used to cold form a thin circular sheet using pressurized gas. The sheet is positioned on a circular die characterized by a radius a and a fillet radius r. In Figure 1, R is the current value of the metal sheet bend radius and h represents the maximum depth reached and measurable at the apex of the formed dome.

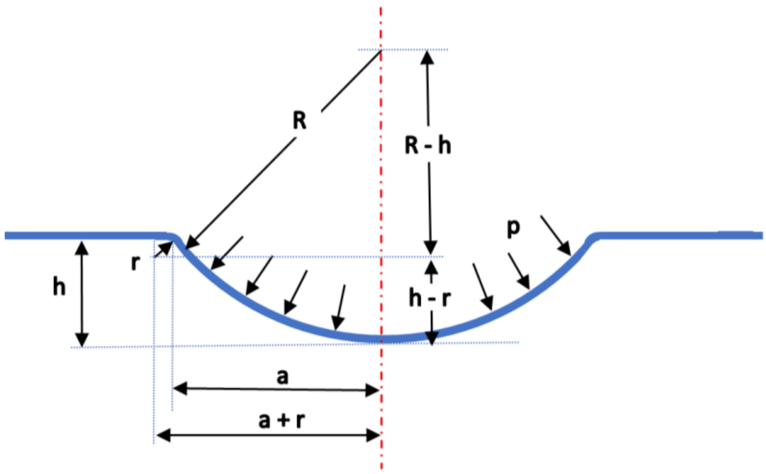

Figure 1. Scheme of the free forming process (in this work "a" was equal to 30 mm and "r" was equal to 2 mm).

To determine the radius of curvature, R, as a function of the geometric parameters of the die and the height at the apex of the dome, the Pythagorean theorem is applied to the triangle constituted by the edges (R + r), [(R − (h − r)] and (a + r):

$$(R+r)^2 = (a+r)^2 + [R-(h-r)]^2 \tag{1}$$

From Equation (1) it can be obtained:

$$R = \frac{(a+r)^2 - r^2 + (h-r)^2}{2h} \tag{2}$$

The developed analytical model is based on the following assumptions:

(1) the material is isotropic;
(2) the elastic deformation is negligible;
(3) the stress along the thickness can be considered zero (the state of stress is biaxial in the whole sheet);
(4) the material is characterized, in the plastic region, by a power law such as:

$$\overline{\sigma} = K\overline{\varepsilon}^n \tag{3}$$

with K the strength coefficient and n the hardening index that should be determined for the material, $\overline{\sigma}$ and $\overline{\varepsilon}$ are, respectively, the stress and the equivalent strain;

(5) the free-forming process is carried out at room temperature;
(6) the formed sheet assumes the shape of the part of a sphere with a curvature radius R.

For the symmetry of the problem, at the pole of the dome, the meridian strain is equal to the circumferential strain. Similarly, for the stress state, an equibiaxial stress state is present at the pole of the dome.

To simplify the formulation, the stress state in the thin sheet subject to free forming is approximated to an equibiaxial plane stress state where $\sigma_r = \sigma_\theta$ and $\sigma_h = 0$ (the subscripts r, θ, and h represent, respectively, the meridian, circumferential, and thickness directions). From the constancy of the volume it is possible to have:

$$\varepsilon_h = -2\varepsilon_r \tag{4}$$

From the Levy–Mises flow law it was obtained that:

$$\bar{\varepsilon} = -\varepsilon_h = ln\left(\frac{s_0}{s}\right) \tag{5}$$

where s_0 and s are initial and current thickness of the sheet, respectively.

From the membrane theory, the equation of the static balance among the forces allows determining the equivalent von Mises stress, using the expression:

$$\bar{\sigma} = \frac{pR}{2s} \tag{6}$$

where p is the applied forming pressure, R is the radius of curvature of the sheet obtained from Equation (2), and s is the current thickness of the sheet.

By carrying out forming tests at different values of the forming pressure and measuring the dome height and thickness at the apex, it is possible to determine pairs of values $\bar{\sigma} - \bar{\varepsilon}$, using the Equations (5) and (6). From the pairs of recorded values, it is possible to trace, through Equation (3), the constants of the material K and n.

4. Experimental Activity

The experimental free-forming activity was carried out on circular discs with a radius of 40 mm and a thickness of 105 μm. The free-forming test was performed using the experimental equipment described in [32] and shown in Figure 2.

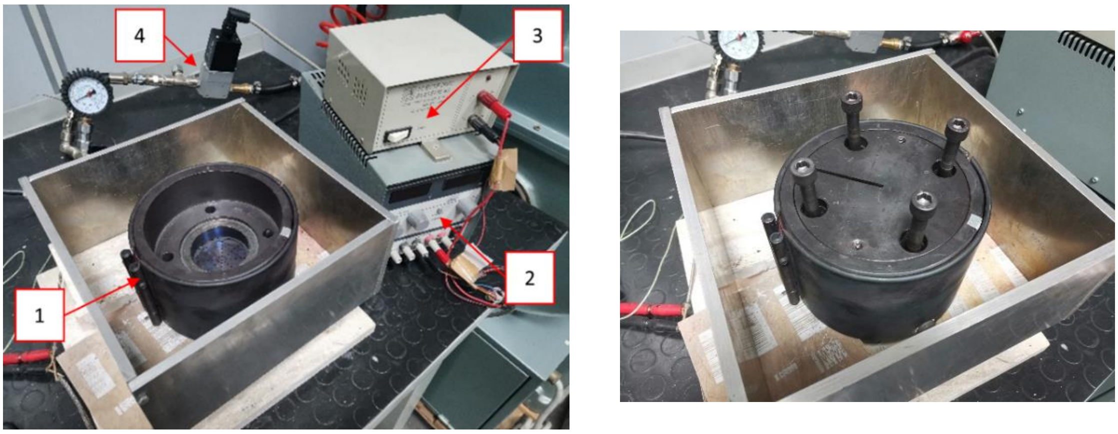

(**a**) (**b**)

Figure 2. Free-forming equipment: (**a**) Constituent elements: die (1), voltage generator (2), stabilizer (3), solenoid valve (4); (**b**) closed die.

The equipment consists of a die divided into two parts. The lower part of the die is characterized by a cavity in which, through the opening of a special solenoid valve, pressurized air enters pushed by a compressor. The upper die, by tightening with four hex head screws, acts as a blank holder, keeping the edges of the sheet constrained to the lower die during the forming process. The screws were fixed using torque wrench with a torque of about 40 Nm. In order to avoid possible misalignment between the die and the blank holder, it has been used a metal gasket between die and specimen. The gasket was made with the same formed material (EA AW 8006 H0), but with a different thickness (200 μm instead 105 μm). In fact, preliminary tests showed that forming the specimens without the metallic gasket could allow the displacement of the specimens between blank holder and die, invalidating the test. The air pressure coming from the compressor is regulated by using a proportional valve connected to a voltage generator. Cold free forming tests were performed at forming pressures of 0.30, 0.35, 0.40, 0.45, and 0.50 MPa. Higher pressure values showed the failure of the specimens, while lower pressures were not investigated because they showed low plastic deformations. Forming tests were realized using a pressure ramp of about 0.1 MPa for minute. In fact, preliminary tests allowed the failure of the specimens if the variation of pressure during forming from room pressure to the target pressure was fast. Once the target values have been reached, the specimens were maintained at that pressure for about 5 min. In another work of the authors [33], the effect of the holding time on the height of the formed domes were investigated. It has been observed that holding time influenced the height of domes but in a negligible way. An example of formed domes is reported in Figure 3.

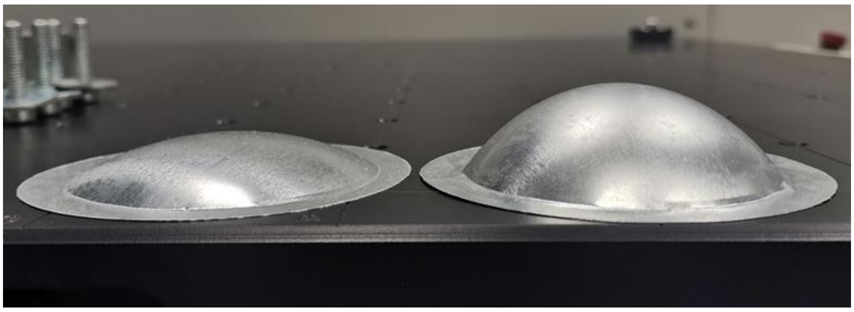

Figure 3. Specimen formed with a pressure of 0.30 MPa (**left**) and specimen formed with a pressure of 0.50 MPa (**right**).

At the end of the forming process, the reached height and the thickness at the apex of the domes are measured. The height of the dome is measured by using an optical profilometer called Conoscan 3000 (produced by Optimet, North Andover, MA, USA), which performs high-precision non-contact measurements giving a three-dimensional scanning of the dome surface (Figure 4) with an accuracy of fewer than 3.0 μm and a repeatability of 0.4 μm. The wavelength of the laser was equal to 685 nm. Conoscopic holography, with respect to other non-contact measurements techniques as triangulations, allowed an optimal acquisition on domes profiles. This was due to the co-linear characteristics of laser beam and sensor, which allowed to measure the points cloud perpendicularly to the surface to be measured. Moreover, the aluminum sheets showed a good reflectance for this laser wavelength. Knowing the range of dome heights, a 75 mm focal lens with a minimum working range of about 18 mm has been adopted. The measurements were made by scanning a square area with the dimensions of 80 mm $\times$ 80 mm. The acquisition of points was in a square grid, while the dimension of the grid were about 50 μm. The acquired point clouds were subsequently subjected to filtering. In the case of 2D analyses, the use of filters allowed the acquired signals to be subdivided into waviness profiles and roughness profiles. Since the aim in this work consisted in measuring the dome heights, the analyses focused on waviness profiles, while roughness profiles were discarded. Because the analyses were carried out not on 2D profiles but on 3D surfaces, the filtering of signals was made according to ISO 25178 using a low pass S-filter with a cut-off wavelength of about 0.08 mm. In this way, it was possible to measure areal waviness parameters (as Sa, Sq, Sz, St, Sv, Ssk, etc.). Once the signals were filtered, they were levelled, in order to avoid incorrect alignments of the specimens during measurements. At this point, the height domes were represented essentially by the Sz parameter, which was simply the maximum height from the highest point to the deepest valley. In order to avoid measurements errors, the boundary part of the point clouds, near the edges of the formed specimens, was manually removed during post-analysis.

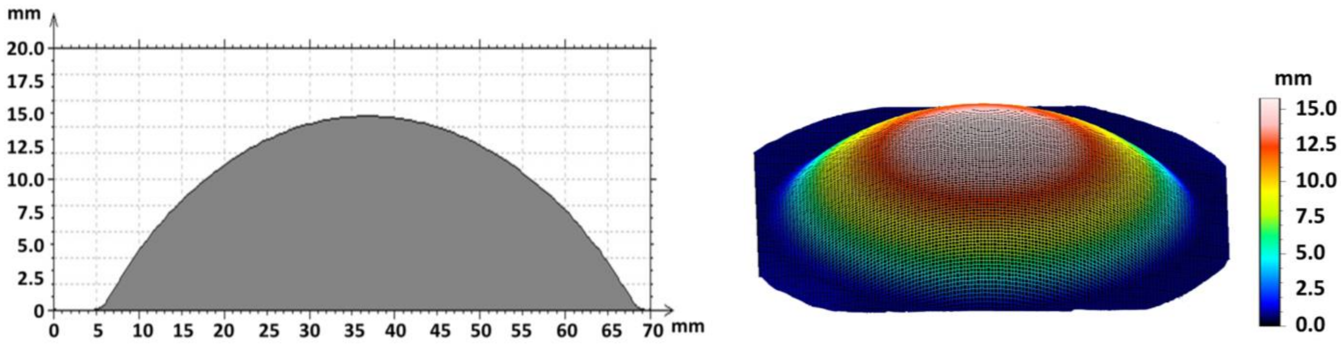

(a) (b)

Figure 4. Scanning of a dome formed with a pressure of 0.50 MPa: (**a**) 2D profile; (**b**) 3D profile.

The measurement of the thickness at the apex of the dome was carried out through the Hall effect thickness gauge Magna-Mike 8600 produced by Olympus Scientific Solutions Americas (MA, USA). The sheet to measure is placed between the magnetic probe and a target consisting of a steel sphere with a diameter of 3.175 mm. Specifically, the probe was fixed on a specific tool while the target was positioned into the cavity of the dome. Subsequently, the dome was manually bright into proximity to the probe: the magnetic field of the probe positioned the target in an optimal way, so as to make the measurement accurately. The instrument allows measuring thicknesses between 1 µm and 6.1 mm with a resolution lower than 5 µm. In Figure 5a,b, it is possible to observe respectively the measurements for a dome thickness formed with a pressure of 0.35 MPa and for a dome thickness formed with a pressure of 0.50 MPa.

(a) (b)

Figure 5. Thickness measurements of dome formed with a pressure of: (**a**) 0.35 MPa; (**b**) 0.50 MPa. (Dimensions in mm).

Table 2 shows the obtained experimental results. As expected, the height of the dome grew as the forming pressure increased, while the dome thickness at the apex decreased.

The average dome height varied from 8.15 mm with a forming pressure of 0.30 MPa to 14.15 mm with a pressure of 0.5 MPa. The increase of dome eight appeared approximative linear until the maximum values of reached pressure. This could be due to a low level of hardening of the investigated material. Observing the measure domes thicknesses, the trend appeared linear, so the increase of domes heights could be due to a major extension of thinning on the formed domes. Moreover, dome height measurements showed an excellent repeatability, with a coefficient of variation (cv) always lower than 1.5%, while the dispersion observed from dome thickness measurements was acceptable and always lower than 6%. The experimental activity has shown that this technology allows plastically deforming very thin thickness aluminum sheets at room temperature in a stable way. The material behavior examined with this technological process can be described by interpolating the acquired experimental results. In fact, putting the data experimentally obtained on forming pressure, height, and thickness at the apex of the dome, which is reported in Table 2, into Equations (2), (5) and (6) the values of R, strain, and stress are obtained. Representing the values of Equations (5) and (6) on a double logarithmic scale, it is easy to obtain the value of *n* and *K*, 0.172 and 157.4 MPa (ln*K* = 5.0587) respectively (Figure 6). The relationship between ln (stress)–ln (strain) is linear with R^2 equal to 0.9991.

Table 2. Experimental results in terms of height and thickness achieved by the sheet under the action of a constant forming gas pressure.

Pressure [Mpa]	Average Dome Height [mm]	Dev. St. Dome Height [mm]	cv Dome Height	Average Dome Thickness [mm]	Dev. St. Dome Thickness [mm]	cv Dome Thickness
0.30	8.15	0.096	1.18%	0.098	0.003	3.06%
0.35	9.31	0.098	1.05%	0.094	0.004	4.26%
0.40	10.61	0.158	1.49%	0.089	0.003	3.37%
0.45	12.46	0.159	1.28%	0.084	0.005	5.95%
0.50	14.51	0.174	1.20%	0.082	0.004	4.88%

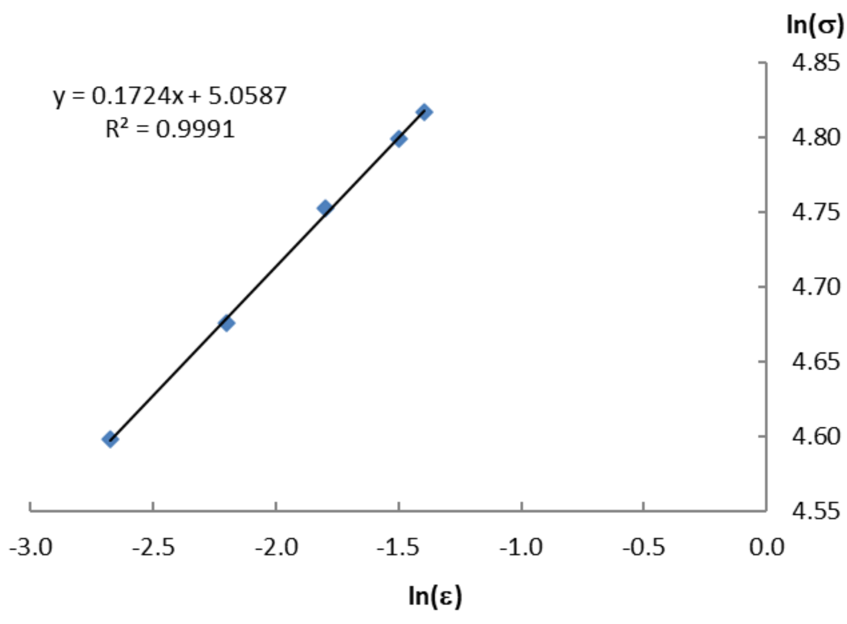

Figure 6. Curve ln (σ) − ln (ε) for the aluminum alloy AA8006.

5. Numerical–Experimental Comparison: Results and Discussions

Introducing the values of n and K obtained through Equations (5) and (6) in a Finite Element Model, it is possible to perform a numerical simulation of the free-forming test.

The free-forming process was numerically simulated through an implicit non-linear finite element code in MSC.Marc environment. The process was schematized as an axisymmetric problem and involves the stretching of a metal sheet subject to the action of a gas under pressure. In particular, as shown in Figure 1, the pressurized gas stretches the sheet metal positioned on a die with an internal diameter of 60 mm and an inlet radius of 2 mm and is constrained to the die edge by a blank holder which avoids its sliding inside the die.

The 2D section of the sheet was discretized through a row of 320 isoparametric and axial symmetric elements with four nodes characterized by bilinear interpolation. The mechanical behavior of the material was simulated through the use of an elastic–plastic model. The von Mises yield criterion and the isotropic hardening law were adopted. The constitutive equation of the material in the plastic field is expressed by the power law of Equation (3). In Equation (3) $\overline{\sigma}$ and $\overline{\varepsilon}$ represent the stress and the equivalent strain, respectively, while K and n are the strength coefficient and the hardening index of the material under study, respectively.

To validate the analytical model of free forming previously described, the K and n constants were introduced in the developed numerical model; then, the numerical model was used to carry out the simulations of the free forming test at different values of the forming pressure.

The die was considered rigid. The problem was characterized by three boundary conditions (Figure 7):

(1) To simulate the presence of the blank holder, the movement of the nodes placed on the edge of the sheet in direct contact with the die was blocked.
(2) The nodes on the outer edge of the sheet, as well as the nodes placed on the symmetry axis, were constrained so as not to move along the direction orthogonal to the symmetry axis.
(3) The gas pressure was applied uniformly to the external edges of the elements.

The forming pressure increases linearly towards the planned pressure value (0.30, 0.35, 0.40, 0.45 and 0.50 Mpa).

Simulation results are shown in Table 3, while a 3D image of the formed dome with a pressure of 0.50 Mpa is reported in Figure 8.

Table 3. Numerical results in terms of height and thickness reached by the sheet under the action of a constant forming gas pressure.

Pressure [MPa]	Numerical Dome Height [mm]	Numerical Dome Thickness [mm]
0.30	8.02	0.094
0.35	9.30	0.091
0.40	10.74	0.086
0.45	12.47	0.080
0.50	14.99	0.071

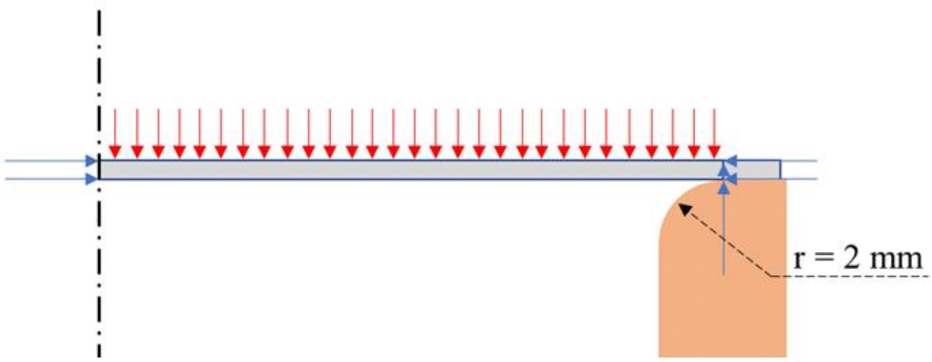

Figure 7. Boundary condition for numerical part: fixed displacements (blue arrows); axis-symmetric condition; imposed pressure on the external edges (red arrows).

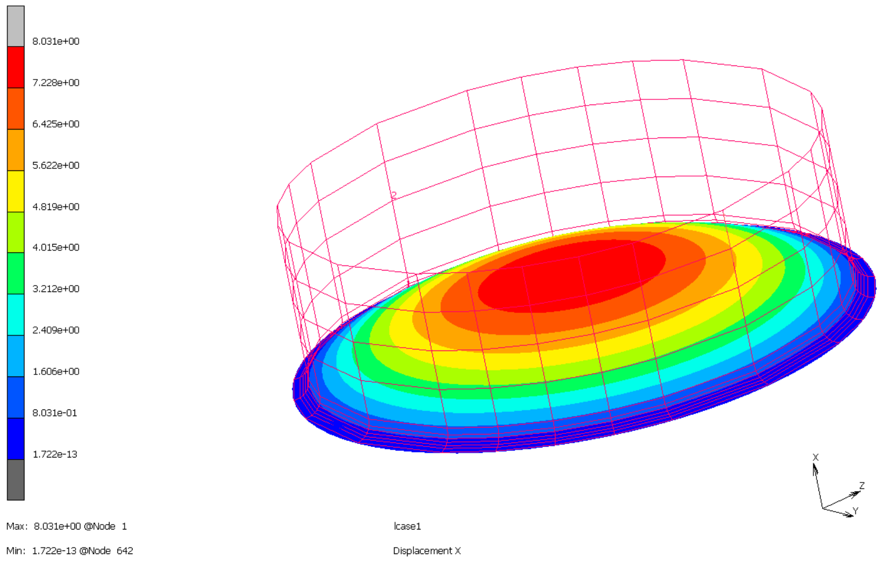

Figure 8. Numeric displacement values along the x axis (vertical direction) obtained with a pressure of 0.50 MPa.

The comparison between numerical and experimental results was carried out in terms of height and thickness reached at the pole of the dome. Table 4 shows the comparison in terms of the percentage difference between the numerical and the experimental results divided by the experimental results. This percentage difference in terms of height at the apex of the dome increases with the pressure remaining under 4%.

Table 4. Numerical–experimental comparison in terms of height and thicknesses reached by the sheet under the action of a constant forming gas pressure.

Pressure [MPa]	Error Dome Height [%]	Error Dome Thickness [%]
0.30	−1.60	−4.08
0.35	−0.11	−3.19
0.40	1.23	−3.37
0.45	0.08	−4.76
0.50	3.31	−13.41

The thickness numerical values measured at the apex of the dome are smaller than the experimental values, the maximum difference is lower than 5%. However, this percentage difference exceeds 13% for forming at a pressure of 0.50 MPa. This may be because, being the specimens close to the breaking pressure, the assumptions of the analytical model differ slightly from the experimental ones. In conclusion, this analysis showed that the numerical results are very accurate for pressures between 0.30 and 0.45 MPa. Therefore, in the hypothesis of material characterized by the power law of Equation (3), it is possible to consider the analytical model previously presented to be adequate for characterization of the behavior of the AA8086 aluminum alloy.

6. Conclusions

In this work AA8006 aluminum alloy thin sheets, generally used in the food packaging sector, were mechanically characterized using the unconventional free forming technique performed at room temperature. Based on the experimental and numerical analyses, the following conclusions can be drawn:

(1) The unconventional blow forming process allows the investigated material to be plastically deformed at room temperature. A maximal pressure value was defined as 0.50 MPa, while pressure values lower than 0.30 MPa were discarded because they

showed negligible plastic deformations. The average dome height increases from about 8.15 mm at 0.30 MPa to 14.51 mm at 0.50 MPa, while average dome thickness decreases from 0.098 mm at 0.30 MPa to 0.082 mm at 0.50 MPa;

(2) The use of a simplified analytical model made it possible to derive the material constants based on a power law. These constants were implemented in a FE model and the comparison between numerical and experimental results confirmed the goodness of the proposed approach with an error in dome height and thickness lower than 5% (except for forming at 0.50 MPa);

(3) The developed approach can constitute an economically effective solution to determine the material constants of a metal sheet under biaxial stresses. In fact, this state of stress reproduces the behavior of the material during the forming process better than the more traditional tensile test, which involves uniaxial stress. Moreover, with the developed approach, the characterization results are not influenced by the cutting technology adopted for specimens manufacturing, which represents a critical aspect in case of manufacturing of very thin metallic specimens.

Author Contributions: Conceptualization, G.G., L.S. and W.P.; methodology, G.G. and G.P.; investigation, G.G. and G.P.; writing—original draft preparation, G.G. and G.P.; writing—review and editing, L.S. and W.P. All authors have read and agreed to the published version of the manuscript.

Funding: This research received no external funding.

Data Availability Statement: All data generated or analyzed during this study are included in this published article.

Conflicts of Interest: The authors declare no conflict of interests.

References

1. Kalpakjian, S.; Schmid, S.R. *Manufacturing Processes for Engineering Materials*; Pearson: London, UK, 2014; ISBN 9788131705667.
2. Lihui, L.; Kangning, L.; Cai, G.; Yang, X.; Guo, C.; Bu, G. A Critical Review on Special Forming Processes and Associated Research for Lightweight Components Based on Sheet and Tube Materials. *Manuf. Rev.* **2014**, *1*, 9. [CrossRef]
3. Sudarsan, C.; Banker, K.H.; Hazra, S.; Bhagat, R.; Panda, S.K. Experimental Investigations on Forming Limit Diagram of Ultra Thin SS 304 Steel: Effect of Circular Grid Size, Sheet Orientation, Punch Size and Deformation Speed. *Adv. Mater. Process. Technol.* **2019**, *5*, 25–38. [CrossRef]
4. Wankhede, P.; Suresh, K. A Review on the Evaluation of Formability in Sheet Metal Forming. *Adv. Mater. Process. Technol.* **2020**, *6*, 402–429. [CrossRef]
5. Kleiner, M.; Geiger, M.; Klaus, A. Manufacturing of Lightweight Components by Metal Forming. *CIRP Ann.-Manuf. Technol.* **2003**, *52*, 521–542. [CrossRef]
6. Cameron, N. *Fundamentals Packaging Technology, Materials and Processes*; Tritech Digital Media: New Delhi, India, 2018.
7. Qian, L.; Paredes, M.; Wierzbicki, T.; Sparrer, Y.; Feuerstein, M. Experimental and Numerical Study on Shear-Punch Test of 6060 T6 Extruded Aluminum Profile. *Int. J. Mech. Sci.* **2016**, *118*, 205–218. [CrossRef]
8. Giuliano, G.; Parodo, G.; Sorrentino, L. Uniformity of Thickness of Metal Sheets by Patchwork Blanks: Potential of Adhesive Bonding. *Frat. Integrità Strutt.* **2020**, *14*, 166–176. [CrossRef]
9. Huang, Y.; Meng, X.; Zhang, Y.; Cao, J.; Feng, J. Micro Friction Stir Welding of Ultra-Thin Al-6061 Sheets. *J. Mater. Process. Technol.* **2017**, *250*, 313–319. [CrossRef]
10. Zhu, M.; Lim, Y.C.; Liu, X.; Cai, Z.; Dhawan, S.; Gao, H.; Politis, D.J. Numerical Forming Limit Prediction for the Optimisation of Initial Blank Shape in Hot Stamping of AA7075. *Int. J. Light. Mater. Manuf.* **2021**, *4*, 269–280. [CrossRef]
11. Ahmed, M.M.Z.; El-Sayed Seleman, M.M.; Ahmed, E.; Reyad, H.A.; Touileb, K.; Albaijan, I. Friction Stir Spot Welding of Different Thickness Sheets of Aluminum Alloy AA6082-T6. *Materials* **2022**, *15*, 2971. [CrossRef]
12. Seleman, M.M.E.S.; Ahmed, M.M.Z.; Ramadan, R.M.; Zaki, B.A. Effect of FSW Parameters on the Microstructure and Mechanical Properties of T-Joints between Dissimilar Al-Alloys. *Int. J. Integr. Eng.* **2022**, *14*, 1. [CrossRef]
13. Giuliano, G. *Superplastic Forming of Advanced Metallic Materials*; Giuliano, G., Ed.; Woodhead Publishing Limited: Sawston, UK, 2011; ISBN 978-1-84569-753-2.
14. Giuliano, G.; Polini, W. Weight Reduction in an AA2017 Aluminum Alloy Part through the Gas Forming Process of a Blank with a Variable Thickness. *Manuf. Technol.* **2021**, *21*, 193–199. [CrossRef]
15. Giuliano, G. On the Constitutive Equation of AA2017 Aluminium Alloy at High Temperature. *Manuf. Lett.* **2016**, *10*, 10–13. [CrossRef]
16. Ayachi, N.; Guermazi, N.; Pham, C.H.; Manach, P.-Y. Development of a Nakazima Test Suitable for Determining the Formability of Ultra-Thin Copper Sheets. *Metals* **2020**, *10*, 1163. [CrossRef]

17. Chang, T.A.; Razali, A.R.; Zainudin, N.A.I.; Yap, W.L. Size Effects in Thin Sheet Metal Forming. *IOP Conf. Ser. Mater. Sci. Eng.* **2015**, *100*, 012051. [CrossRef]
18. Trost, C.O.W.; Wurster, S.; Freitag, C.; Steinberger, A.; Cordill, M.J. A New Approach to Evaluate the Elastic Modulus of Metallic Foils. *Mater. Des.* **2020**, *196*, 109149. [CrossRef]
19. Pandey, A.K.; Date, P.P. Mechanical and Micro-Structural Characterization of Hot Rolled Brass Foil. *Mater. Charact.* **2021**, *181*, 111515. [CrossRef]
20. Sorrentino, L.; Parodo, G.; Giuliano, G. Lightweight Structures: An Innovative Method to Uniform the Thickness of Metal Sheets by Patchwork Blanks. *Int. J. Light. Mater. Manuf.* **2022**, *5*, 20–28. [CrossRef]
21. Prakash, V.; Kumar, D.R. Performance Evaluation of Bio-Lubricants in Strip Drawing and Deep Drawing of an Aluminium Alloy. *Adv. Mater. Process. Technol.* **2020**, *8*, 1044–1057. [CrossRef]
22. Ahmed, M.; Shrivastava, A.; Kumar, D.R.; Nabi, M.U.; Ahmed, M.; Shrivastava, A.; Kumar, D.R.; Un, M. Optimisation of Process Parameters for Energy- Efficient Electro-Hydraulic Forming of Al-Mg Alloy Sheets. *Adv. Mater. Process. Technol.* **2020**, *6*, 620–636. [CrossRef]
23. Jovane, F. An Approximate Analysis of the Superplastic Forming of a Thin Circular Diaphragm: Theory and Experiments. *Int. J. Mech. Sci.* **1968**, *10*, 403–424. [CrossRef]
24. Yang, H.S.; Mukherjee, A.K. An Analysis of the Superplastic Forming of a Circular Sheet Diaphragm. *Int. J. Mech. Sci.* **1992**, *34*, 283–297. [CrossRef]
25. Cornfield, G.C.; Johnson, R.H. The Forming of Superplastic Sheet Metal. *Int. J. Mech. Sci.* **1970**, *12*, 479–488. [CrossRef]
26. Holt, D.L. An Analysis of the Bulging of a Superplastic Sheet by Lateral Pressure. *Int. J. Mech. Sci.* **1970**, *12*, 491–497. [CrossRef]
27. Hwang, Y.M.; Yang, J.S.; Chen, T.R.; Huang, J.C. Analysis of Superplastic Sheet-Metal Forming in a Circular Closed-Die Considering Non-Uniform Thinning. *J. Mater. Process. Technol.* **1997**, *65*, 215–227. [CrossRef]
28. Giuliano, G.; Franchitti, S. The Determination of Material Parameters from Superplastic Free-Bulging Tests at Constant Pressure. *Int. J. Mach. Tools Manuf.* **2008**, *48*, 1519–1522. [CrossRef]
29. Giuliano, G. Constitutive Equation for Superplastic Ti-6Al-4V Alloy. *Mater. Des.* **2008**, *29*, 1330–1333. [CrossRef]
30. Gillo, G. *AZ31 Magnesium Alloy Parameters Identification through Inverse Analysis at 713 K*; Trans Tech Publications Ltd: Bäch, Switzerland, 2012; Volume 504–506, ISBN 9783037853665.
31. Giuliano, G. Constitutive Modelling of Superplastic AA-5083. *Tech. Mech.* **2012**, *32*, 221–226.
32. Giovinco, G.; Giuliano, G.; Testa, G.; Barlat, F.; Moon, Y.H.; Lee, M.G. Forming Apparatus to Investigate the Effect of Temperature on the Superplastic Behaviour of Alloys. In Proceedings of the AIP Conference Proceedings, Chonburi, Thailand, 18–20 July 2018; Volume 1252, pp. 304–311.
33. Giuliano, G.; Parodo, G.; Polini, W. Cold Blow Forming of a Thin Sheet in AA8006 Aluminum Alloy. *Eng. Sci. Res. J.* **2023**, *23*. [CrossRef]